7C.4 WIND, WAVES AND LANGMUIR CIRCULATION DURING CBLAST-LOW

Albert J. Plueddemann *
Woods Hole Oceanographic Institution, Woods Hole, Massachusetts

1. INTRODUCTION

As a part of the 2003 Coupled Boundary Layers and Air-Sea Transfer Low-Wind Experiment (CBLAST-Low), surface winds, surface waves, upper-ocean structure, and Langmuir circulation strength were observed with instrumentation deployed at the Martha's Vineyard Costal Observatory (MVCO) and the CBLAST Air-Sea Interaction Tower (ASIT), located to the south of the island (Fig.1). Varying wind directions relative to Martha's Vineyard create a complex wave field at the site, which may include growing, short-fetch wind waves and decaying wind waves along with persistent swell from the south. Data from various sources were used to estimate wave parameters associated with these wave field components. The strength and dominant scale of Langmuir circulation were determined from a Fanbeam ADCP that measured the horizontal structure of near-surface velocity at scales from 10-100 m. The relationship between observed Langmuir circulation strength and surface forcing was explored, with particular attention to the variation in circulation strength with wind speed, wind direction, and wave age.

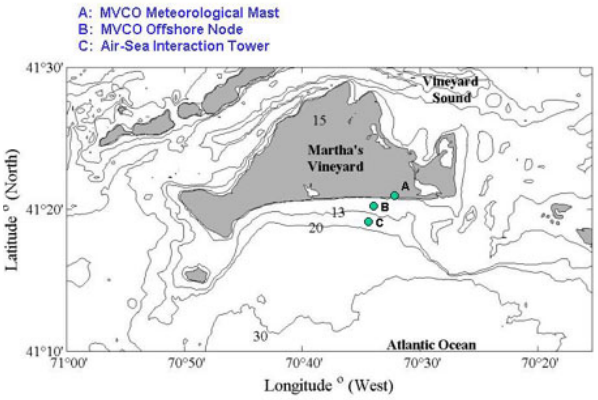

Figure 1. The CBLAST-Low study region.

* *Corresponding author address:* Al Plueddemann, Woods Hole Oceanographic Institution, 202A Clark Lab, MS-29, Woods Hole, MA 02543-1541; email: aplueddemann@whoi.edu.

2. CBLAST-LOW OBSERVATIONS

The observations reported here were obtained during 13 days (16 – 28 Aug) of the CBLAST-Low intensive observing period in the summer of 2003. Wind observations were available from both the MVCO meteorological mast (location "A" in Fig. 1) and the ASIT mast about 3.2 km south of Martha's Vineyard (Fig. 1 "C"). The ASIT winds, observed by sonic anemometers at multiple heights on the ASIT, were used in this study. Wind speeds were adjusted from the measurement height to a standard height of 10 m and combined to form a continuous record (J. Edson, personal communication).

Wave height data were available from a laser altimeter on the ASIT and from a near-bottom pressure gauge deployed just south of the ASIT (15 m water depth). A bottom-mounted ADCP at the MVCO offshore node (Fig. 1 "B"; 12 m water depth) provided directional wave data. Water column stratification was measured with a string of temperature-conductivity (T-C) sensors below the ASIT. The MVCO ADCP was used to estimate surface wave directional spectra from orbital velocities measured in the near-surface bins of each beam. After pre-processing and comparison of wave heights to those from the altimeter and pressure sensor, the ADCP directional spectra were further analyzed to separate swell and locally forced wind waves using the method of Hanson and Phillips (2001).

The Fanbeam ADCP (Plueddemann et al., 2001) was deployed on a bottom lander along with a current meter, T-C sensor and pressure sensor. The bottom lander consisted of a steel frame with a 1 x 1.6 m footprint and a sled-like bottom, which allows the frame to slide along the seafloor during deployment and recovery. The Fanbeam ADCP was cabled to the ASIT node, and from there connected through to the MVCO node, making power and internet data transfer available.

The unique transducer head configuration of the Fanbeam ADCP results in beams that are broad in elevation, but narrow in azimuth. The beams are directed towards the sea surface from below at a shallow angle. For wind speeds greater than about

3 m/s, the acoustic backscatter is dominated by microbubbles in the upper few meters of the water column (e.g., Crawford and Farmer, 1987), and each beam effectively maps out a horizontal profile of near-surface current. Processing of the along-beam velocities allows Langmuir circulation to be detected (Smith, 1992; 1998, Plueddemann et al., 1996; 2001).

3. WIND VARIABILITY

Surface forcing conditions during the observation period varied from negligible wind stress and strong thermal forcing to modest wind speeds (3–10 m/s) where wave breaking and Langmuir circulations were expected to play a role in air-sea exchange processes. The majority of winds were from the SW quadrant at 3-7 m/s, whereas the weakest winds were from the SE (Fig. 2). The strongest winds were from the NW, but these events were short lived compared to those from the SW.

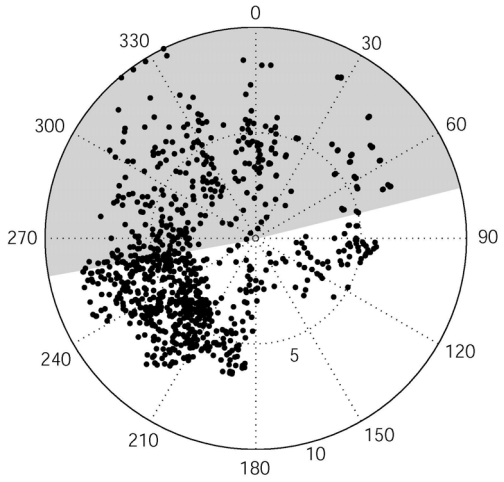

Figure 2. Wind speed (m/s) and direction at the ASIT during 16–28 August 2003. Gray shaded area represents directions from which the island of Martha's Vineyard shelters the ASIT site.

The proximity of the ASIT to Martha's Vineyard results in short fetch (~20 km) for winds from the W and very short fetch (3-10 km) for winds from the N to ENE (Fig. 1). Wind directions for which the island shelters the site from wind waves (260^0 – 75^0) are shown in gray in Fig. 2. In addition, shallow water and the presence of Nomans Land Island off the SW tip of Martha's Vineyard limit wave development from the WSW (245^0 – 260^0).

4. THE WAVE FIELD

The CBLAST-Low site is exposed to the open ocean to the S, but surrounded by Martha's Vineyard to the N, Nantucket Island to the E and the New England coastline to the W. As expected, swell was predominantly from the south. Further examination showed a distinction between relatively weak, long period swell from distant Atlantic storms and stronger, shorter-period swell associated with decaying wind waves from local wind events. The former were predominantly from the SSE, the latter from the SSW. Significant wave height (SWH) was < 0.5 m for the long-period swell and up to 1 m for short-period swell.

The wind sea at the site was strongly influenced by the presence of Martha's Vineyard (Fig. 3). Wind sea directions were tightly clustered in the SW quadrant between 180^0 and 245^0. The fact that only a handful of wind seas were detected within the sheltered region (detection thresholds for the MVCO ADCP were about 0.1 m SHW and 2.5 sec period) was attributed to the short fetch from these directions. The lack of a strong wind sea response in the SE quadrant may have been because the wind events tended to be weaker and more rapidly varying in direction compared to those in the SW quadrant. The weak wind sea in the SW quadrant between 245^0 – 260^0, despite relatively strong, persistent winds, is attributable to Nomans Land and the SW shoals of Martha's Vineyard.

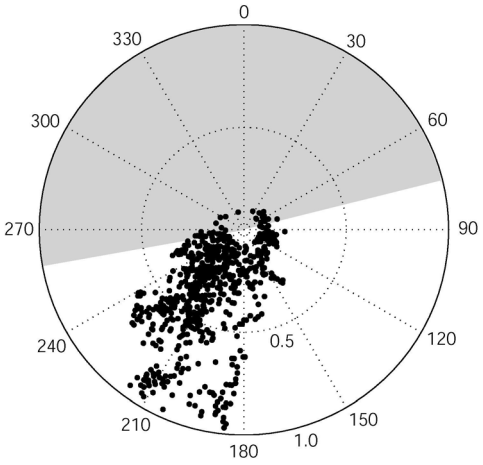

Figure 3. Significant wave height (m) and direction for the wind sea at the MVCO seanode. Shading is the same as in Fig. 2.

The SWH of the wind sea varied from below the detection threshold to about 1 m. Although wind sea and swell were of similar amplitude, they could often be separated based on frequency. However, in some situations wind sea and swell frequencies overlapped and in other cases (e.g. increasing wind speed following a rapid change in direction from previously steady winds) the spectrum contained a growing wind sea, a decaying wind sea and a swell peak. The availability of directional spectra was critical to separating wave field components in these situations.

5. LANGMUIR CIRCULATION

For the purposes of detecting Langmuir circulation with the Fanbeam ADCP, surface velocity profiles obtain-ed at 1 sec intervals were averaged to 1 min and the range-mean velocity was subtracted from each beam for each time step. In the presence of Langmuir circulation, the range-dependent velocity for the beam oriented most nearly cross-wind will be alternately convergent and divergent as successive cells are en-countered. The Langmuir cells are also advected by the large-scale current, causing the converg-ence zones to migrate in range with time, and resulting in a sequence of ``bands'' in a time-range plot of the velocity anomaly.

Figure 4 shows such a time-range plot during a 30 min period on 19 August when Langmuir circ-ulation was well developed. Wind speed was about 5 m/s from the WSW, and the local wind sea was just developing in the presence of a decaying swell from the south. Bands of alternating positive and negative velocity vs. range from the trans-ducer indicate convergence and divergence. Migration of the bands with time is due to advection by the mean flow. The translation speed of about 8 cm/s away from the transducer inferred from the angle of the bands is consistent with both the range-mean Fanbeam velocity and the velocity in the direction of the beam deduced from a nearby current meter. The dominant scale (distance between convergence zones) is about 20 m, consistent with a mixed layer depth of about 7 m for cells with a 1.5:1 (width:depth) aspect ratio (Smith, 1992; 1998).

To the extent that Langmuir circulation dominates the velocity anomaly field, the root mean-square velocity along the beam, Vrms, provides an estimate of circulation strength (Plueddemann at al., 1996; Smith, 1998). For the results described here, we compute Vrms as the average value in a 20 min interval for the beam oriented most nearly cross-wind. For Fig. 4 the peak velocity anomalies are 4-6 cm/s and Vrms ~ 2 cm/s.

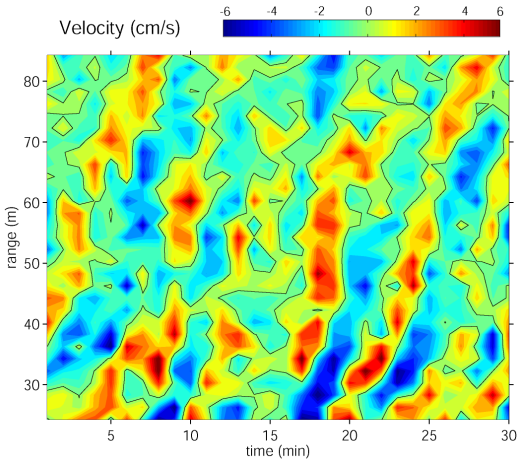

Figure 4. Time-range plot of velocity anomaly from the crosswind beam of the Fanbeam ADCP near noon UTC on 19 August.

Modulation of Langmuir circulation strength during CBLAST-Low appears to be strongly related to wind direction, emphasizing the role of Martha's Vineyard in controlling wind sea development. The state of wave development can be parameterized using the wave age Cp/u*, where Cp is the phase speed of the locally-forced wind waves and u* is the atmospheric friction velocity. Developing, short-fetch wind waves will have a relatively low wave age (e.g. 20), whereas well developed wind seas will have age near 30 and decaying wind sea or swell may have age from 50 to several hundred.

The complexity of the interactions among wind, waves and Langmuir circulation is illustrated in Fig. 5. During a ~15 hour period on 19 August, wind speed increases from < 2 m/s to > 8 m/s and then remains relatively steady (Fig. 5a). Although SWH based on the spectral peak remains flat during the period of wind growth, separation into wind sea and swell (Fig. 5b) shows that this is due to the combined affect of decaying swell and a growing wind sea. The wind sea is first detected at 1200 h and builds until early on 20 August, sur-passsing the height of the swell at 2200 h.

Wave age based on the wind sea (Fig.5c) indicates developing waves from 1200 to 2400 h, followed by a transition to well developed seas. Wave age based on the spectral peak frequency does not correctly represent the state of develop-

ment until the wind sea dominates the spectrum after 2200 h.

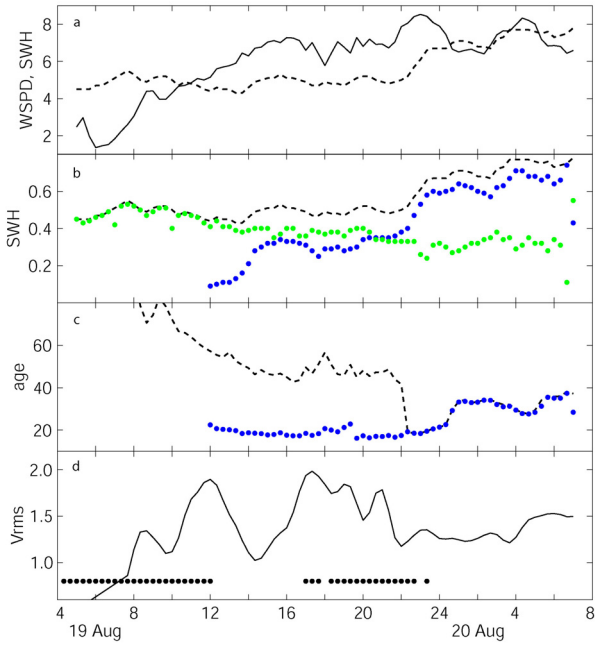

*Figure 5. a) Wind speed (solid) and 10*SWH of the spectral peak (dashed), b) SWH separated into wind sea (blue) and swell (green) components, c) Wave age based on the peak period (black) and the wind sea period (blue), d) Langmuir circulation strength as measured by Vrms from the Fanbeam ADCP. Dots indicate wind directions that are not subject to sheltering by Martha's Vineyard. The banded structures shown in Fig. 4 were associated with the Vrms peak at 1200 h.*

Increasing Vrms after 0800 h (Fig. 5d) indicates development of Langmuir circulation, presumably in the presence of wind seas too weak to be detected in the ADCP directional spectra. Vrms peaks at 1200 h, after which there is a conspicuous trough followed by a second peak at about 1700 h. The reduction of circulation strength is unexpected given the persistent wind and wave growth and low wave age. The explanation for the trough (as well as the reduction in Vrms after 2200 h) appears to be the changing wind direction. Initially from the SW, the wind rotates clockwise past 245^{o} between 1200 and 1700 h and after 2300 h.

Langmuir circulation strength is expected to scale as the product of u* and the Stokes drift Us (e.g. Vrms = $[u^*]^a[Us]^b$) but the most appropriate parameterization has not been determined. The scaling has been examined in only a few observational studies (Smith, 2001) and the results have been ambiguous because u* and Us are strongly co-varying for fully developed seas. Despite complexities due to sheltering, further examination of the CBLAST-Low observations is of interest because the coastal setting results in a wide range of wave development and increases the likelihood of separating the influence of u* and Us in the scaling.

ACKNOWLEDGMENTS

Jim Edson and John Trowbridge made CBLAST-Low and the ASIT a reality. Edson provided the meteorological data used in this study. R. Krishfield was responsible for field deployment of the Fanbeam ADCP. The APL Waves analysis pack-age, run by J. Churchill, provided the directional wave parameters. This work was supported by the Office of Naval Research, Grants N00014-01-1-0129 and N00014-03-1-0681.

REFERENCES

Crawford, G.B. and D.M. Farmer, 1987. On the spatial distribution of ocean bubbles, *J. Geophys. Res*., **92** (C8), 8231--8243.

Hanson, J. L. and O. M. Phillips, 2001: Automated analysis of ocean surface directional wave spectra. *J. Atmos. Oceanic Technol*., **18**, 277–293.

Smith, J.A., 1992. Observed growth of Langmuir circulation, *J. Geophys. Res*., **97**(C4), 5651--5664.

Smith, J.A., 1998. Evolution of Langmuir circulation during a storm, *Journal of Geophysical Research, 103*(C1), 12,649-12,668.

Smith, J.A., 2001. Observations and theories of Langmuir circulation: A story of mixing, In *Fluid Mechanics and the Environment: Dynamical Approaches*, J.L. Lumley, Ed., 295-314, Springer, New York.

Plueddemann, A.J., J.A. Smith, D.M. Farmer, R.A. Weller, W.R. Crawford, R. Pinkel, S.Vagle and A. Gnanadesikan, 1996. Structure and variability of Langmuir circulation during the Surface Waves Processes Program, *J. Geophys. Res*., **101**(C2), 3525-3543.

Plueddemann, A.J., E.A. Terray and R. Merewether, 2001. Design and performance of a self-contained, fan-beam ADCP, *IEEE J. Oceanic Eng*., **26**(2), 252-258.